

Smooth self-energy in the exact-diagonalization-based dynamical mean-field theory: Intermediate-representation filtering approach

Yuki Nagai¹ and Hiroshi Shinaoka²

¹CCSE, Japan Atomic Energy Agency, 178-4-4, Wakashiba, Kashiwa, Chiba, 277-0871, Japan

²Department of Physics, Saitama University, Saitama 338-8570, Japan

(Dated: December 14, 2024)

We propose a method for obtaining converged smooth real-frequency self-energy as a function of a discretized bath number in the dynamical mean-field theory with the finite-temperature exact diagonalization (DMFT-ED). One of the benefits of conventional DMFT-ED calculations is that one can obtain real-frequency spectra without a numerical analytical continuation. However, it is hard to understand the physical meaning of these spectra, since these spectra are spiky and positions of spikes strongly depend on the number of the bath sites. On the other hand, it is known that the Matsubara Green's function, which can be calculated from the spiky spectra, is converged as a function of a discretized bath number. We show that the sparseness of the imaginary-time quantities explains these differences. With the use of the intermediate representation (IR) basis of the self-energy, we show the DMFT-ED calculation can give converged smooth self-energy with only four bath sites. Our IR-filtering approach makes the DMFT-ED scheme controllable as a function of the number of the bath sites.

Introduction Strongly correlated electron systems have attracted much attention in the past 30 years, because of the discovery of interesting materials such as high temperature superconductors or heavy fermions. These materials have rich phase diagrams, which have superconducting, magnetic, or Mott insulating phases. New theoretical schemes and techniques have been developed to understand many-body physics due to correlation between electrons in condensed matter physics.

The dynamical mean-field theory (DMFT) is one of the most powerful tools to take strong correlations into account[1]. The DMFT is used both in calculations with model Hamiltonians and in realistic electronic structure calculations[2]. Within the DMFT, local dynamical correlations are fully preserved while the spatial correlations are neglected. Under this approximation, one has to solve an effective Anderson impurity model mapped from an original lattice model. The mapping onto the impurity model is enforced by a self-consistency condition which contains the information about the original lattice. Recently, it is known that the continuous-time quantum Monte Carlo method is one of the powerful “exact” impurity solvers since there is no discretization of the imaginary-time interval[3]. One needs, however, to perform numerical analytical continuation to transform calculated imaginary-time quantity to real-frequency spectra, which is extremely sensitive to noise. This is because the self-energy is computed in Matsubara frequency domain and must be continued to the real frequency axis. QMC calculations also suffer from a negative sign problem at low temperature in solving cluster-type and multi-orbital impurity problems.

The exact diagonalization is another powerful “exact” and “sign-problem-free solver” for the effective impurity model[1, 4]. This ED technique can be combined with DMFT as the finite temperature exact di-

agonalization method (DMFT-ED). In this method, the self-consistent procedure is still implemented on the Matsubara-frequency axis. In solving an impurity model, its continuous bath is discretized with a finite number of bath sites. Solving this approximate finite-size system by ED, one can directly calculate Green's functions and self-energies on the real-frequency axis without unstable numerical analytical continuation, which is an advantage of the DMFT-ED.

However, the real-frequency quantities such as spectral functions and self-energies have spiky structures, whose positions strongly depend on the number of the bath sites. On the other hand, DMFT-ED calculations actually give almost equivalent results for Matsubara/imaginary-time quantities to those of QMC-based DMFT calculations only with a few bath sites[4]. The strong bath-site dependence of the real-frequency quantities makes it difficult to interpret the physical meanings of their fine features. Thus, there is a demand for a method to obtain converged results for the real-frequency quantities. Another fundamental question is why the real-frequency quantities converge much slowly than the imaginary-time ones.

In this paper, we propose a method for obtaining *bath-number-insensitive* converged smooth self-energies from the results of DMFT-ED calculations. Recently, it was shown that the imaginary-time/Matsubara Green's functions are sparse at finite temperature: the imaginary-time/frequency dependence of these Green's functions can be represented by a few dozen basis functions of the so-called intermediate representation (IR) basis [5–8]. In the previous study[5], they used this representation together with sparse modeling (SpM) techniques in data science to extract noise-insensitive spectral functions from QMC data[5]. Using the IR, in the present study, we clarify the difference between quantities on

imaginary Matsubara and real frequencies in DMFT-ED calculations. In particular, we use the IR-filtering approach to obtain the bath-number-insensitive spectrum in DMFT-ED calculations. Then, we apply the present method to single-site DMFT calculations. We find that low-order coefficients of the self-energy in terms of the IR basis are converged with respect to the number of sites. We demonstrate that the physically-relevant smooth self-energies can be obtained with only four bath sites from these converged coefficients. This indicates that the bath-site-dependent higher orders of the IR basis of the self-energy can be regarded as noises from discretization errors. Finally, we show the physically-relevant real-frequency smooth self-energy in the DMFT-ED calculation, which is difficult to obtain in the QMC method. Our IR-filtering approach makes the DMFT-ED scheme controllable as a function of the number of the bath sites. The present method will be further improved by using the SpM techniques.

Sparseness of the self-energy The DMFT method maps a lattice model onto an effective impurity model. Figure 1 illustrates the DMFT-ED self-consistent cycle for finite T . The self-consistent equation reads

$$G_{\text{loc}}(i\omega_n) = G_f(i\omega_n), \quad (1)$$

where $G_{\text{loc}}(i\omega_n)$ and $G_f(i\omega_n)$ are the local Matsubara temperature Green's functions of the original and effective impurity models, respectively. Here, we consider fermion Matsubara frequencies $\omega_n = \pi T(2n + 1)$ with $n = 0, \pm 1, \dots, \pm n_{\text{max}}$ (n_{max} is typically larger than 10^3). As revealed in the previous studies [5, 6, 8], however, $G_{\text{loc}}(i\omega_n)$ and $G_f(i\omega_n)$ actually contain much fewer degrees of freedom than n_{max} .

The real-frequency self-energy is computed as

$$\Sigma^R(\omega) \equiv \mathcal{G}_0^R(\omega)^{-1} - G^R(\omega)^{-1}, \quad (2)$$

$G^R(\omega)$ and $\mathcal{G}_0^R(\omega)$ are full and non-interacting retarded Green's functions for the effective impurity model, respectively. In the present study, we will clarify how much information is contained in this real-frequency self-energy.

In the previous study [5, 6], they considered an exact integral equation between the Matsubara Green's function $G(i\omega_n)$ and the spectral function $\rho(\omega)$ (i.e. Lehmann representation),

$$G(i\omega_n) = \int_{-\infty}^{\infty} d\omega K^F(i\omega_n, \omega) \rho(\omega), \quad (3)$$

where $K^F(\omega_n, \omega) \equiv 1/(i\omega_n - \omega)$ for fermions.

In the present study, we focus on a similar spectral representation for the self-energy [11]:

$$\Sigma(i\omega_n) = \Sigma_{\text{const}} + \int_{-\infty}^{\infty} d\omega K^F(i\omega_n, \omega) \rho^{\Sigma}(\omega), \quad (4)$$

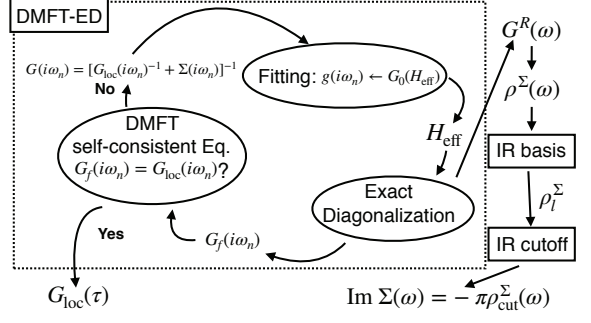


FIG. 1. Schematic figure of the calculation process to obtain the smooth self-energy $\Sigma(\omega)$ in the DMFT-ED calculation.

$$\Sigma(i\omega_n) \xleftarrow[\text{Lehmann rep.}]{\Sigma(i\omega_n) - \Sigma_0 = \int d\omega K^F(i\omega_n, \omega) \rho^{\Sigma}(\omega)} \rho^{\Sigma}(\omega) = -\frac{1}{\pi} \text{Im} \Sigma^R(\omega)$$

$$\Sigma_l \xleftarrow[\text{Lehmann rep.}]{\Sigma(i\omega_n) - \Sigma_0 = \sum_l \Sigma_l U_l^F(i\omega_n)} \rho_l^{\Sigma} \xleftarrow[\text{Projection}]{\rho_l^{\Sigma} = \sum_l \rho_l^{\Sigma} V_l^F(\omega)} \Sigma_l = -S_l \rho_l^{\Sigma}$$

FIG. 2. Relation between different representations of the self-energy.

where $\rho^{\Sigma}(\omega) (\equiv -\pi^{-1} \text{Im}(\Sigma^R(\omega)))$ is a spectral function and Σ_{const} is a frequency-independent term. Although $\rho^{\Sigma}(\omega)$ is a spiky bath-number-dependent function in the DMFT-ED framework, $\Sigma(i\omega_n)$ computed by Eq. (4) is a smooth function. This is because the model-independent filter matrix $K(i\omega_n, \omega)$ smears out fine features in $\rho^{\Sigma}(\omega)$.

This can be clearly seen by expanding these quantities in terms of “intermediate representation” (IR) basis [6, 8] as

$$\Sigma(i\omega_n) - \Sigma_{\text{const}} = \sum_{l=0}^{\infty} \Sigma_l U_l^F(i\omega_n), \quad (5)$$

$$\rho^{\Sigma}(\omega) = \sum_{l=0}^{\infty} \rho_l^{\Sigma} V_l^F(\omega). \quad (6)$$

These basis functions are defined through the decomposition of the kernel as [6, 8]

$$K^F(i\omega_n, \omega) = -\sum_{l=0}^{\infty} S_l^F U_l^F(i\omega_n) V_l^F(\omega), \quad (7)$$

The basis functions are orthonormalized in the intervals of $n \in [-\infty, +\infty]$ and $[-\omega_{\text{max}}, \omega_{\text{max}}]$, respectively (ω_{max} is a cutoff frequency). Note that the real part of the self-energy $\text{Re}(\Sigma^{\text{Re}}(\omega))$ can be computed from $\rho^{\Sigma}(\omega)$ by the Kramers-Kronig relation.

If ω_{max} is large enough to cover the support of the

spectrum, ρ_l^Σ and Σ_l are related (see Fig. 2) as

$$\Sigma_l = -S_l^F \rho_l^\Sigma. \quad (8)$$

Because the singular values S_l^F ($l = 0, 1, 2, \dots$) decay exponentially, in numerical calculations with double precision floating point numbers, any Green's functions and self-energies can be represented by only few $U_l(i\omega_n)$ corresponding to large singular values (i.e. $S_l/S_0 > 10^{-8}$). In the present study, we use $\beta = 1/T = 20$ and $\omega_{\max} = 5$. This leaves only 25 ($= l_{\max}$) singular values.

The above consideration indicates that the Green's functions in Eq. (1), and hence the real-frequency self-energy, have few independent variables no more than l_{\max} , which does not depend on details of the model. As clarified below, this explains why the Matsubara Green's function converges to that obtained by QMC calculation with a small number of bath sites in DMFT-ED calculations [4].

On the basis of the concept of the IR, we may obtain a converged solution *only if the variables of the effective Hamiltonian is more than the number of singular values S_l required for a desired accuracy*. The effective impurity Hamiltonian reads

$$H_{\text{AIM}} = \sum_{l\sigma} \epsilon_{l\sigma} c_{l\sigma}^\dagger c_{l\sigma} + \sum_{l\sigma} V_{l\sigma} (f_\sigma^\dagger c_{l\sigma} + c_{l\sigma}^\dagger f_\sigma) + H_{\text{atomic}}, \quad (9)$$

where H_{atomic} the on-site atomic part of the original Hamiltonian. For example, the Hubbard model has $H_{\text{atomic}} = -\mu \sum_\sigma f_\sigma^\dagger f_\sigma + U f_\uparrow^\dagger f_\uparrow f_\downarrow^\dagger f_\downarrow$. Here, f_σ^\dagger and $c_{l\sigma}$ are creation operators for fermions in with spin σ associated with the impurity site and with the state l of the effective bath, respectively. Thus, the effective impurity Hamiltonian involves N_s independent parameters ($\epsilon_{l\sigma}$ and $V_{l\sigma}$).

Physically-relevant converged self-energy Now we test our idea and propose a method for obtaining a physically-relevant smooth spectrum which is converged as a function of N_s . In particular, we consider a half-filled single-band Hubbard model with the semicircular density of states $\rho_0(\omega) = [2/(\pi D) \sqrt{1 - (\omega/D)^2}]$ as the original lattice model. We set the half bandwidth D as the energy unit. In particular, we focus on metallic and insulating solutions obtained for $U = 2D$ and $2.4D$, respectively. For the present model, $\Sigma_{\text{const}} = 0$ due to particle-hole symmetry.

Figure 3 and 4 show the computed $\text{Im}(\Sigma(i\omega_n))$ and $\rho^\Sigma(\omega)$ ($= -\frac{1}{\pi} \text{Im} \Sigma^R(\omega)$), respectively. As clearly seen, $\text{Im}(\Sigma(i\omega_n))$ is a smooth function, being bath-site-number independent. In contrast, $\rho^\Sigma(\omega)$ computed by Eq. (2) has spiky structures, which strongly depend on the number of the bath sites (not shown).

To obtain a deeper insight into this contrasting behavior, we compute their expansion coefficients in the IR using Eqs. (5) and (6). Figure 5 compares Σ_l and ρ_l^Σ

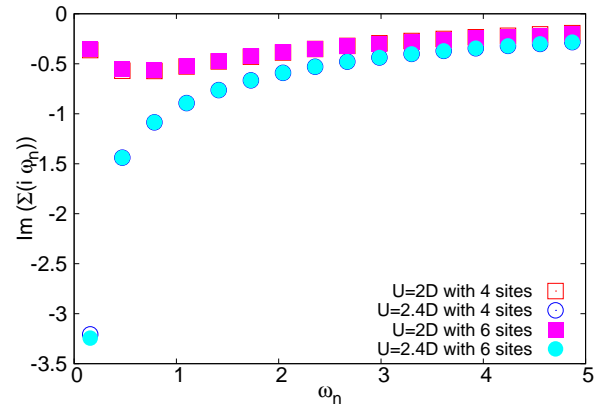


FIG. 3. (Color online) Imaginary part of the self-energy on the Matsubara frequency axis $\text{Im}(\Sigma(i\omega_n))$ with $U = 2D$ and $U = 2.4D$ after the 200 loops of the DMFT-ED calculation with 4 site baths. We consider $\beta = 20$, $\omega_{\max} = 5$, $n_{\max} = 1024$ in the half-filled Hubbard model with the semicircular density of states with a half bandwidth D .

computed with $N_s = 4, 8, 10$ for $U = 2D$. As clearly seen in Fig. 5(a), ρ_l^Σ does not vanish as l is increased. Furthermore, the large- l components strongly depends on N_s . On the other hand, Σ_l decay exponentially with respect to l . We obtained converged results for Σ_l ($l \leq 8$) only with four bath sites[10], while the small coefficients at larger l fluctuate with respect to N_s . This originates from the discretization of the bath. These small discretization errors in Σ_l are amplified and propagate to ρ_l^Σ through Eq. (8), leading to the large fluctuations of ρ_l^Σ at large l . This strongly indicates that the bath-site-dependent (spiky) component of the spectral function originates from tiny discretization errors in the Green's function. Thus, they *are not* physically relevant in the finite-temperature DMFT calculation based on the Matsubara Green's function.

By truncating the expansion at $l = l_{\text{cut}}$ (IR filtering), we obtain smooth self-energies on real frequency axis as shown in Fig. 4. With the use of these self-energies, we can understand difference between systems with $U = 2D$ and $U = 2.4D$. Note that the imaginary part of the self-energy is the inverse of the quasiparticle lifetime. In the case of $U = 2D$, the density of states should have a peak at the zero energy since the imaginary part of the self-energy at zero energy is zero, which suggests that this system is metallic. In the case of $U = 2.4D$, there is no intensity of the density of states at the zero energy since there is a strong quasiparticle dumping at the zero energy, which suggests that this system is in the Mott insulating phase. We note that the self-energy on the real-frequency axis is also useful for the non-hermitian topological theory in finite-temperature strongly-correlated systems[12–14]. The DMFT-ED calculation with the IR basis gives us physically relevant information which does

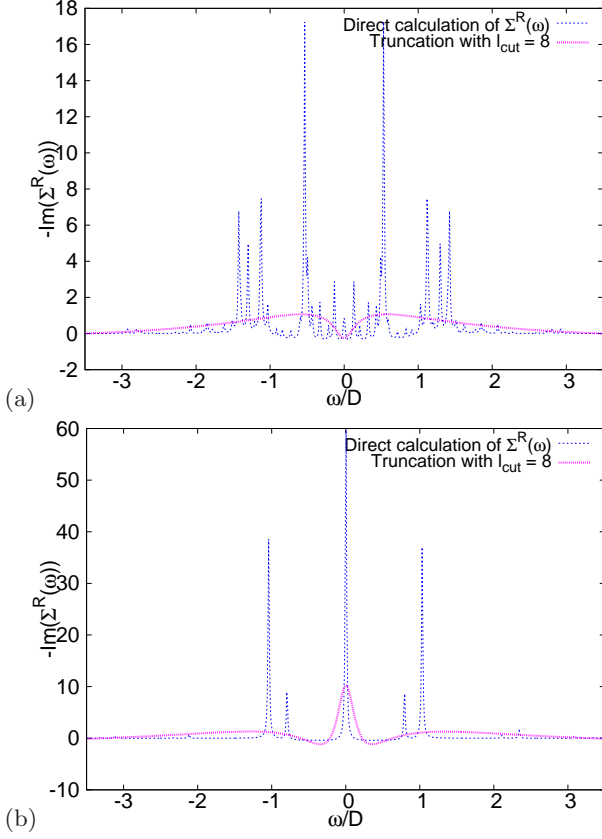


FIG. 4. (Color online) Imaginary part of the self-energy $\text{Im}\Sigma^R(\omega)$ calculated by the direct calculation in the DMFT-ED, and the truncation with $l_{\text{cut}} = 10$ with (a) $U = 2D$ and (b) $U = 2.4D$. We consider 4 bath sites. Other parameters are the same as in Fig. 3.

not depend on the number of the bath sites.

We note that the present method can be further improved by using the SpM techniques. As shown in Fig. 4(b), the self-energy with the truncation $l_{\text{cut}} = 8$ has the non-causal region ($-\text{Im}\Sigma^R(\omega) < 0$) around $|\omega| = 0.3D$, which may be ascribed to Gibbs oscillations due to the truncation. We confirm that the self-energy with the truncation $l_{\text{cut}} = 6$ is causal. To obtain smooth and causal self-energies, we can use the SpM techniques which was originally used to realize a stable analytical continuation of imaginary-time Green's functions based on the IR basis [5]. This approach will allow us to obtain a solution which satisfies non-negativity $\rho^\Sigma(\omega) > 0$ for the self-energy. In the previous paper [5], they proposed to use the SpM approach for obtaining a noise-insensitive spectrum from QMC data. In the present study, by assuming that the components with $l > l_{\text{cut}}$ are ‘noise’ due to the finite bath size, we use this method to obtain the bath-number-insensitive spectrum. Once one obtains a smooth causal imaginary part of the self-energy, the real part of the self-energy can be obtained by the Kramers-

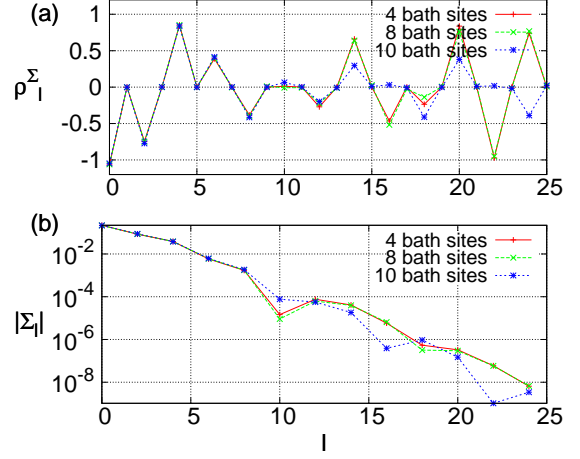


FIG. 5. (Color online) Bath-site-number dependence of the coefficients ρ_l^Σ and $|\Sigma_l|$ of IR basis after the 200 loops of the DMFT-ED calculation. Other parameters are the same as in Fig. 3.

Kronig relation.

Discussions With the use of the IR basis, we can discuss whether the number of the bath sites is enough or not. In cluster or multi-orbital DMFT-ED calculations, the number of the bath sites is usually limited to a small number. In these cases, one can discuss a validity by comparing two systems with different number of the bath sites.

At finite temperature, the DMFT and imaginary-time Green function-based methods have maximally l_{cut} information, since the kernel $K(i\omega_n, \omega)$ is a model-independent function. An energy resolution of a spectral function is determined by the temperature and spectral width. Even if the number of the bath sites is extremely large, the resolution of the Matsubara Green's function in Eq. (1) is limited by the minimum singular value $s_l > \delta$. In terms of the data science, there might be an over-fitting problem when the number of the bath site is much larger than the number of the effective singular values, since one needs to fit the sparse Matsubara Green's function to obtain the coefficients of the effective impurity Hamiltonian.

We summarize our procedure to obtain the smooth bath-site-insensitive function $\Sigma^R(\omega)$ in the DMFT-ED calculation, as shown in Fig. 1. First, we conventionally converge the DMFT loops with desired accuracy of the self-consistency equations with different bath sizes. In the DMFT-ED calculation, the imaginary-time and Matsubara Green's functions $G(\tau)$ and $G(i\omega_n)$, spiky spectral functions $\rho(\omega)$, and spiky self-energy $\Sigma(\omega)$ are obtained. We compute the expansion coefficients in terms of the IR basis functions ρ_l^Σ and Σ_l . If the functions ρ_l^Σ and Σ_l with $l \leq l_{\text{cut}}$ are converged as a function of the number of the bath sites, we can obtain the smooth bath-site-insensitive

self-energy $\Sigma^R(\omega)$ by introducing the IR filtering with a truncation at l_{cut} . The smooth causal spectral function of the self-energy $\rho^\Sigma(\omega)$ can be also calculated by the SpM-based analytical continuation[5]. We should note that, in the DMFT-ED calculation, there is no statistical error and no negative sign-problem, which appear in the QMC calculation.

Summary In this work, we introduce the IR-filtering approach to obtain the physically relevant self-energies, which do not depend on the number of the bath sites in the DMFT-ED calculation. The IR basis is useful to analyze the convergence of the DMFT-ED calculations. This approach can be extended to the multi-orbital or cluster DMFT schemes, since the kernel $K(i\omega_n, \omega)$ does not depend on the details of models and methods. The present method will be further improved by using the SpM techniques in data science.

Acknowledgment Y. N. would like to acknowledge S. Yamada for helpful discussions and comments about the exact diagonalization technique. H. S. thanks S. Sakai, J. Otsuki, K. Yoshimi, N. Chikano for fruitful discussions. We use “rbasis 0.1.7”, a Python library for the intermediate representation (IR) basis functions[9]. The rbasis is called in the Julia language 0.6.2. The calculations were partially performed by the supercomputing systems SGI ICE X at the Japan Atomic Energy Agency. Y. N. was partially supported by JSPS KAKENHI Grant Number 18K11345 and 18K03552, the “Topological Materials Science” (No. JP18H04228) KAKENHI on Innovative Areas from JSPS of Japan. HS was supported by JSPS KAKENHI Grants No. 16H01064 (J-Physics), 18H04301 (J-Physics), 16K17735, 18H01158.

Phys. Rev. B **96**, 035147 (2017).

- [7] H. Shinaoka, J. Otsuki, K. Haule, M. Wallerberger, E. Gull, K. Yoshimi, and M. Ohzeki, Overcomplete compact representation of two-particle Green’s functions, Phys. Rev. B **97**, 205111 (2018).
- [8] N. Chikano, J. Otsuki, H. Shinaoka, Performance analysis of physically constructed orthogonal representation of imaginary-time Green’s function, arXiv:1803.07257 (unpublished).
- [9] N. Chikano, K. Yoshimi, J. Otsuki, H. Shinaoka (unpublished), url: <https://pypi.org/project/rbasis/>
- [10] See Supplemental Material at [URL will be inserted by publisher for the technical details of the DMFT-ED calculation.]
- [11] J. M. Luttinger, Analytic Properties of Single-Particle Propagators for Many-Fermion Systems, Phys. Rev. **121**, 942 (1961).
- [12] H. Shen, B. Zhen, and L. Fu, Topological Band Theory for Non-Hermitian Hamiltonians, Phys. Rev. Lett. **120**, 146402 (2018).
- [13] V. Kozii, L. Fu, Non-Hermitian Topological Theory of Finite-Lifetime Quasiparticles: Prediction of Bulk Fermi Arc Due to Exceptional Point, arXiv:1708.05841.
- [14] Y. Nagai, Y. Qi, H. Isobe, V. Kozii, and L. Fu, in preparation.

- [1] A. Georges, G. Kotliar, W. Krauth and M. J. Rozenberg, Dynamical mean-field theory of strongly correlated fermion systems and the limit of infinite dimensions, Rev. Mod. Phys. **68**, 13 (1996).
- [2] G. Kotliar, S. Y. Savrasov, K. Haule, V. S. Oudovenko, O. Parcollet, and C. A. Marianetti, Electronic structure calculations with dynamical mean-field theory, Rev. Mod. Phys. **78**, 865 (2006).
- [3] E. Gull, A. J. Millis, A. I. Lichtenstein, A. N. Rubtsov, M. Troyer, and P. Werner, Continuous-time Monte Carlo methods for quantum impurity models, Rev. Mod. Phys. **83**, 349 (2011).
- [4] M. Capone, L. de Medici, and A. Georges, Solving the dynamical mean-field theory at very low temperatures using the Lanczos exact diagonalization, Phys. Rev. B **76**, 245116 (2007).
- [5] J. Otsuki, M. Ohzeki, H. Shinaoka, and K. Yoshimi, Sparse modeling approach to analytical continuation of imaginary-time quantum Monte Carlo data, Phys. Rev. E **95**, 061302(R) (2017).
- [6] H. Shinaoka, J. Otsuki, M. Ohzeki, and K. Yoshimi, Compressing Green’s function using intermediate representation between imaginary-time and real-frequency domains,

Supplemental material

S1. Details of the finite-temperature dynamical mean field theory with the exact diagonalization solver

The DMFT method maps a lattice model onto an effective impurity model written as

$$H_{\text{AIM}} = \sum_{l\sigma} \epsilon_{l\sigma} c_{l\sigma}^\dagger c_{l\sigma} + \sum_{l\sigma} V_{l\sigma} (f_{\sigma}^\dagger c_{l\sigma} + c_{l\sigma}^\dagger f_{\sigma}) + H_{\text{atomic}}, \quad (\text{S1})$$

where H_{atomic} the on-site atomic part of the original Hamiltonian. For example, the Hubbard model has $H_{\text{atomic}} = -\mu \sum_{\sigma} f_{\sigma}^\dagger f_{\sigma} + U f_{\uparrow}^\dagger f_{\uparrow} f_{\downarrow}^\dagger f_{\downarrow}$. Here, f_{σ}^\dagger and $c_{l\sigma}$ are creation operators for fermions in with spin σ associated with the impurity site and with the state l of the effective bath, respectively.

The self-consistent equation in the DMFT framework is written as

$$G_{\text{loc}}(i\omega_n) = G_f(i\omega_n), \quad (\text{S2})$$

where $G_{\text{loc}}(i\omega_n)$ is the local Matsubara Green's function of the original Hamiltonian defined as

$$G_{\text{loc}}(i\omega_n) = \int d\epsilon D(\epsilon) [i\omega_n + \mu - \epsilon - \Sigma(i\omega_n)]^{-1}. \quad (\text{S3})$$

The momentum-independent self-energy $\Sigma(i\omega_n)$ is calculated by the Dyson equation for the effective impurity model:

$$\Sigma(i\omega_n) \equiv \mathcal{G}_0^{-1}(i\omega_n) - G_f^{-1}(i\omega_n). \quad (\text{S4})$$

Here, $\mathcal{G}_0(i\omega_n)$ is a non-interacting part of the Green's function for the effective impurity model calculated as

$$\mathcal{G}_0^{-1}(i\omega_n) = i\omega_n + \mu - \sum_l^{N_s} \frac{|V_l|^2}{i\omega_n - \epsilon_l}. \quad (\text{S5})$$

The impurity Green's function is calculated as

$$G_{f,\sigma}(i\omega_n) = -\frac{1}{Z} \sum_k e^{-\beta E_k} G_{\sigma}^{(k)}(i\omega_n), \quad (\text{S6})$$

where

$$\begin{aligned} G_{\sigma}^{(k)}(i\omega_n) &= \langle k | f_{\sigma} [i\omega_n - (H_{\text{AIM}} - E_k)]^{-1} f_{\sigma}^\dagger | k \rangle \\ &+ \langle k | f_{\sigma}^\dagger [i\omega_n + (H_{\text{AIM}} - E_k)]^{-1} f_{\sigma} | k \rangle. \end{aligned} \quad (\text{S7})$$

Here, $Z = \sum_k e^{-\beta E_k}$ is a partition function and E_k and $|k\rangle$ is an k -th eigenstate and eigenvalue of H_{AIM} , respectively. The local density of states is expressed as

$$\rho_{\sigma}(\omega) = \frac{1}{Z} \sum_k e^{-\beta E_k} (1/\pi) \text{Im} G_{\sigma}^{(k)}(i\omega_n \rightarrow \omega + i\eta). \quad (\text{S8})$$

At each DMFT step, we fit the parameters ϵ_l and V_l to reproduce $\mathcal{G}_0(i\omega_n)$, calculate the impurity Green's function $G_{f,\sigma}(i\omega_n)$, and calculate the non-interacting Green's function $\mathcal{G}_0(i\omega_n) = [G_{f,\sigma}(i\omega_n)^{-1} + \Sigma(i\omega_n)]^{-1}$ for next step.

S2. Green's function obtained by the exact diagonalization technique at finite temperature

We describe how to calculate Green's function as follows. To calculate the impurity Green's function, we obtain the eigenvalues and eigenvectors of H_{AIM} . In the Hubbard model, the Hamiltonian matrix H_{AIM} is block diagonal since the spin-number is conserved in each block matrices. Thus, the Green's function is expressed as

$$G_{f,\sigma}(i\omega_n) = -\frac{1}{Z} \sum_{n_{\uparrow}=0}^{N_s+1} \sum_{n_{\downarrow}=0}^{N_s+1} \sum_l e^{-\beta E_{n_{\uparrow},n_{\downarrow}}^l} G_{\sigma}^{(n_{\uparrow},n_{\downarrow},l)}(i\omega_n), \quad (\text{S9})$$

where

$$G_{\uparrow}^{(n_{\uparrow}, n_{\downarrow}, l)}(i\omega_n) = \langle (n_{\uparrow}, n_{\downarrow}, l) | f_{\uparrow}[i\omega_n - (H_{\text{AIM}}^{n_{\uparrow}+1, n_{\downarrow}} - E_{n_{\uparrow}, n_{\downarrow}}^l)]^{-1} f_{\uparrow}^{\dagger} | (n_{\uparrow}, n_{\downarrow}, l) \rangle \\ + \langle (n_{\uparrow}, n_{\downarrow}, l) | f_{\uparrow}^{\dagger}[i\omega_n + (H_{\text{AIM}}^{n_{\uparrow}-1, n_{\downarrow}} - E_{n_{\uparrow}, n_{\downarrow}}^l)]^{-1} f_{\uparrow} | (n_{\uparrow}, n_{\downarrow}, l) \rangle. \quad (\text{S10})$$

$$G_{\downarrow}^{(n_{\uparrow}, n_{\downarrow}, l)}(i\omega_n) = \langle (n_{\uparrow}, n_{\downarrow}, l) | f_{\downarrow}[i\omega_n - (H_{\text{AIM}}^{n_{\uparrow}, n_{\downarrow}+1} - E_{n_{\uparrow}, n_{\downarrow}}^l)]^{-1} f_{\downarrow}^{\dagger} | (n_{\uparrow}, n_{\downarrow}, l) \rangle \\ + \langle (n_{\uparrow}, n_{\downarrow}, l) | f_{\downarrow}^{\dagger}[i\omega_n + (H_{\text{AIM}}^{n_{\uparrow}, n_{\downarrow}-1} - E_{n_{\uparrow}, n_{\downarrow}}^l)]^{-1} f_{\downarrow} | (n_{\uparrow}, n_{\downarrow}, l) \rangle. \quad (\text{S11})$$

Here, N_s is the number of bath sites, and n_{\uparrow} and n_{\downarrow} are numbers of up and down spins, respectively. $H_{\text{AIM}}^{n_{\uparrow}, n_{\downarrow}}$ is the Hamiltonian matrix with fixed n_{\uparrow} and n_{\downarrow} . $E_{n_{\uparrow}, n_{\downarrow}}^l$ and $|(n_{\uparrow}, n_{\downarrow}, l)\rangle$ are the l -th eigenvalues and eigenvectors associated with $H_{\text{AIM}}^{n_{\uparrow}, n_{\downarrow}}$. In this paper, we use eigs in the Julia language 0.6.2, which computes eigenvalues and eigenvectors using implicitly restarted Lanczos iterations for real symmetric matrix. The diagonal element of the inverse of the matrix $\langle (n_{\uparrow}, n_{\downarrow}, l) | f_{\uparrow}[i\omega_n - (H_{\text{AIM}}^{n_{\uparrow}+1, n_{\downarrow}} - E_{n_{\uparrow}, n_{\downarrow}}^l)]^{-1} f_{\uparrow}^{\dagger} | (n_{\uparrow}, n_{\downarrow}, l) \rangle$ is calculated by the Lanczos method[1]. In all calculations in main text, we consider 4 eigenvalues and eigenvectors in each block diagonal Hamiltonian $H_{\text{AIM}}^{n_{\uparrow}, n_{\downarrow}}$.

[1] A. Georges, G. Kotliar, W. Krauth and M. J. Rozenberg, Dynamical mean-field theory of strongly correlated fermion systems and the limit of infinite dimensions, Rev. Mod. Phys. **68**, 13 (1996).